Physica D 239 (2010) 1048 1060

Contents lists available at ScienceDirect

Physica D

journal homepage: www.elsevier.com/locate/physd

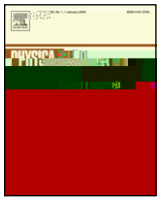

Stability of bumps in piecewise smooth neural fields with nonlinear adaptation

Zachary P. Kilpatrick [a], Paul C. Bressloff [b,]

[a] *Department of Mathematics, University of Utah, Salt Lake City, UT 84112, USA*

[b] *Mathematical Institute, University of Oxford, 24-29 St. Giles', Oxford OX1 3LB, UK*

a r t i c l e i n f o

Article history:
Received 7 December 2009
Received in revised form
23 February 2010

when the weight distribution $w(x)$ is given by a so-called Mexican hat function with the following properties: $w(x) > 0$ for $x \in [0, x_0)$ with $w(x_0) = 0$; $w(x) < 0$ for $x \in (x_0, 1]$; $w(x)$ is decreasing on $[0, x_0]$; $w(x)$ has a unique minimum on $\mathbb{R}^+$ at $x = x_1$ with $x_1 > x_0$ and $w(x)$ strictly increasing on $(x_1, 1]$. On the other hand, in the case of a purely excitatory network with $w(x)$ a positive, monotonically decreasing function, any bump solution is unstable and tends to break up into a pair of counterpropagating fronts. Following Amari's original analysis, the study of bumps in

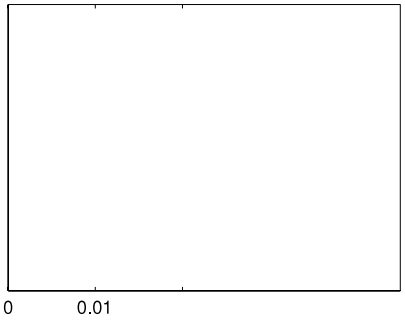

Fig. 1. Stationary bumps in a network with synaptic depression. (a) Plots relating bump width a to amplitude of synaptic depression for different values of using Eq. (2.6). We take the parameter D 20. Stability analysis based on the piecewise smooth approach (Section 2.3) establishes that bumps along the dashed portions of the existence curves are unstable; the solid curves indicate bumps that appear to be numerically stable. The Evans function approach predicts that the whole of the upper branch is stable. (b) Bump profile when D 0:2 and D 0:01.

state solution for $U(x)$ and evaluating the integral yields

$$U(x) = \frac{1}{(1 +)} \left[e^{-|x+a|} - e^{-|x-a|} \right] :$$

Applying the threshold conditions $U(a) =$, we arrive at an implicit expression relating the bump half-width a to all other parameters:

$$\frac{2a}{(1 +)} e^{-2a} = :$$

The transcendental equation (2.6) can be solved numerically using a root finding algorithm. The variation of pulse width with the parameters and is shown in Fig. 1; the stability of the bumps is calculated below. It is important to note that the threshold-crossing conditions (2.6) are necessary but not sufficient for existence of a bump. A rigorous proof of existence, which establishes that activity is superthreshold everywhere within the domain $|x| < a$ and subthreshold for all $|x| > a$, has not been obtained except in special cases [6]. However, it is straightforward to check numerically that these conditions are satisfied.

2.2. Stability of bumps: Evans function approach

A popular approach to analyzing the stability of stationary bumps in neural field models is to linearize about the bump solution and derive an Evans function, whose roots represent the spectrum of the associated linear system [10]. Thus, it is tempting to try to calculate the Evans function of the bump solutions (2.6), find its roots, and use these to make statements about the linear stability of the bump. However, the steps necessary to linearize the system (2.1) when f D are not well defined, due to the exposed Heaviside function in Eq.

The resulting spectral problem

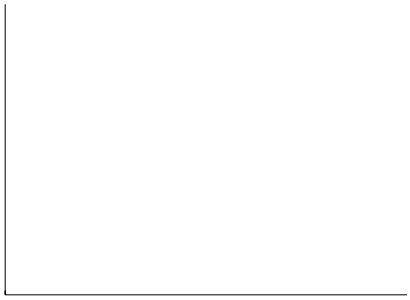

Fig. 2. Eigenvalues associated with respect to shift perturbations (cases (i) and (ii)). (a) Nonzero eigenvalue for various

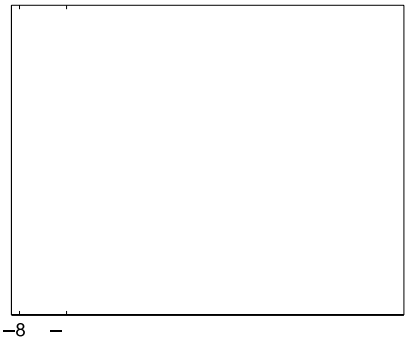

Fig. 4. Stationary bump in a network with spike frequency adaptation. (a) Bump solution $(U(x), H(x))$ with $h_0 = 0.04$, $= 0.1$, and $= 0.16$. Here $a = 1.48$, $b = 1.60$, and $c = 1.67$. (b) Zoomed in version of the excited region RTU, showing all of the threshold crossings at $x = a, b, c$.
Source: Adapted from [

Fig. 6. Different sized perturbations of a bump. (a) Expanding a side of the bump. Zoomed-in version of the bump $.U.x/; H.x//$ is shown along with perturbed solutions $u_1.x/ \mathrm{D} U.x/ \mathrm{C} {}_1.x/$ and $u_2.x/ \mathrm{D} U.x/ \mathrm{C} {}_2.x/$ with ${}_i.x/ > 0$. While u_1 satisfies the three threshold crossings on this side, u_2 does not, due to the condition $u_2.a \mathrm{C} {}^{a}_{C}/ \mathrm{D} h_0 \mathrm{C}$ being violated. (b) Contracting a side of the bump. Here, $u_1.x/ \mathrm{D} U.x/ {}_1.x/; . {}_1.x/ > 0/$ still satisfies all three threshold crossing, but $u_2 \mathrm{D} U {}_2; . {}_2 > 0/$ does not, due to $u_2.c \mathrm{C} {}^{C}_{c}/ \mathrm{D} h_0$ being violated. Parameters are h_0 D 0:04, D 0:1, D 0:16.

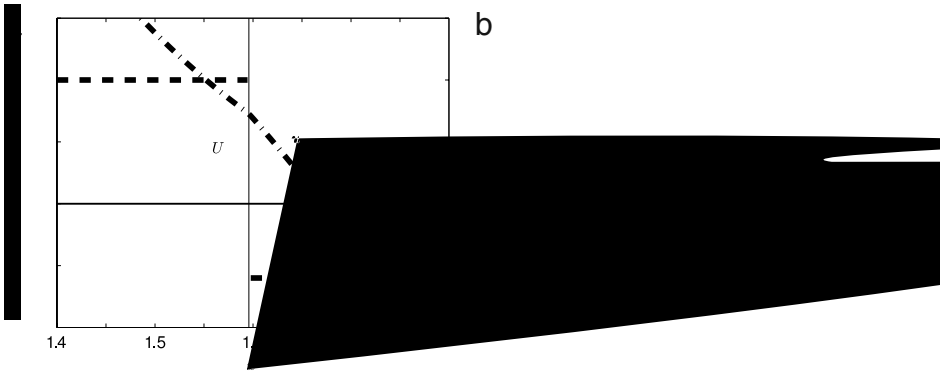

Fig. 7. Effects of perturbations on the excited region $R\overline{U}\cup$. (a) Zoomed-in version of the bump $U.x/; H.x/$ shows the accompanying excited region $R\overline{U}\cup$ (black bar). Expanding a side of the bump to the perturbed form $u_1.x/ \mathrm{D} U.x/ \mathrm{C} {}_1.x/; . {}_1 > 0/$ will widen both subdomains of the excited region $R\overline{u_1}\cup$ (grey bars). (b) Contracting a side of the bump to the perturbed form $u_1.x/ \mathrm{D} U.x/ {}_1.x/; . {}_1 > 0/$ shrinks both subdomains of the excited region $R\overline{u_1}\cup$ (grey bars). Parameters are h_0 D 0:04, D 0:1, D 0:16.

where $g.x/ \mathrm{D} xe^{\mathrm{jxj}}$. Also note

$$H.x/ \mathrm{D} \begin{cases} h_0 \mathrm{C} \ ; & \mathrm{jxj} > b; \\ h_0; & \mathrm{jxj} < b; \end{cases} \tag{3.7}$$

implying that, as in the case of the network with depression, the negative feedback variable here will have a jump discontinuity. Applying the bump threshold conditions (3.4) (3.6), we arrive at an implicit system relating the bump half-widths $a; b; c$ to all other parameters

$$\begin{aligned} &g.a \mathrm{C} c/ \quad g.a \mathrm{C} b/ \mathrm{C} g.2a/ \mathrm{C} g.a \quad b/ \quad g.a \quad c/ \mathrm{D} h_0 \mathrm{C} \ ; \\ &g.b \mathrm{C} c/ \quad g.2b/ \mathrm{C} g.b \mathrm{C} a/ \quad g.b \quad a/ \quad g.b \quad c/ \mathrm{D} \ ; \\ &g.2c/ \quad g.c \mathrm{C} b/ \mathrm{C} g.c \mathrm{C} a/ \quad g.c \quad a/ \mathrm{C} g.c \quad b/ \mathrm{D} h_0: \end{aligned} \tag{3.8}$$

The system of transcendental equations (3.8) can be solved numerically using a root finding algorithm. The variation of pulse width with the parameters and h_0 is shown in Fig. 5. The stability of the bumps is calculated below.

3.2. Stability of bumps

As in the case of networks with sy425(sy425ith)-521insy425(sy425ith)-521d [(/)]TJ/F150 9.5641 Tf 5.6'hesys.me0 .4 RG with sy

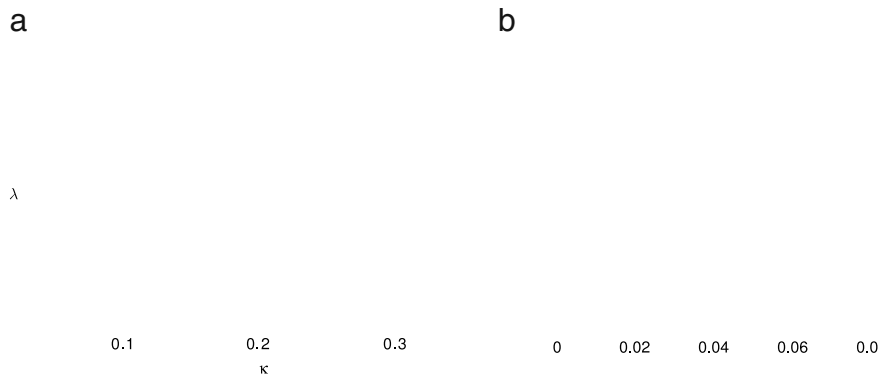

Fig. 8. Plot of eigenvalues arising from perturbations of a bump solution as a function of (a) with h_0 D 0:04, and (b) h_0 with D 0:16. In both plots, the positive eigenvalue associated with a shift perturbation is always larger than that associated with an expansion/contraction. Other parameters are D 0:1 and D 1. Varying has the effect of merely scaling the eigenvalues, but not changing their sign.

$$u.\ b\,C\ {}^{b}.t/;t/\ D\ ; \qquad (3.11)$$
$$u.\ c\,C\ {}^{c}.t/;t/\ D\ h.\ c\,C\ {}^{c}.t/;t/;$$

for an initial time interval following the perturbation t 2 .0; T/. The linear theory will only be valid until the time T that the existence threshold conditions are violated. It is straightforward to Taylor expand the expressions in (3.11), truncate to first order in , and solve for the terms

$$\begin{aligned} {}^{a}.t/ &\quad \frac{.\ a;t/\ \ '.\ a;t/}{\mathrm{j}U^{0}.a/\mathrm{j}};\\ {}^{b}.t/ &\quad \frac{.\ b;t/}{\mathrm{j}U^{0}.b/\mathrm{j}}; \qquad (3.12)\\ {}^{c}.t/ &\quad \frac{.\ c;t/\ \ '.\ c;t/}{\mathrm{j}U^{0}.c/\mathrm{j}}: \end{aligned}$$

It is important to note that an infinitesimal shift of the point at which u crosses is not equivalent to shifting the boundary of the outer region of the excited region of u, due to the discontinuity in $H.x/$. As shown in Fig. 7, infinitesimal perturbations of the bump lead to changes in the excited region of u in a neighborhood of x D $a;\ c$ but not x D a

Fig. 9. Instabilities of a stationary bump solution given by Eqs. (3.6) and (3.7). (a) Space time plot of a bump destabilizing to form a traveling pulse for D 1:0; D 0:16. The activity $u.x; t/$ evolves from an initial bump solution that is perturbed by a small rightward shift at t D 5. (b) Space time plot of a bump destabilizing to form a spatially localized breather for D 1:2; D 0:16. The activity $u.x; t/$ evolves from an initial bump solution that is perturbed by an expansion at t D 5. Other parameters are D 0:1, h_0 D 0:04.

$$\mathbf{M} \mathrm{D} \begin{pmatrix} 0 & \\ & \end{pmatrix}$$

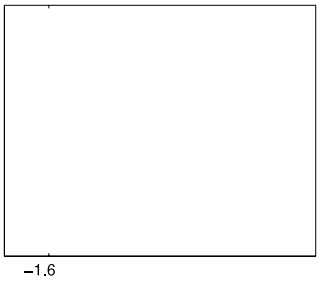

Fig. 10. Snapshots of a bump destabilizing to a traveling pulse at successive times t D 5; 5:5; 6; 10 (top to bottom) for D 1:0, and D 0:16. Both $u.x; t/$ (solid black curves) and $h.x; t/$ (black squares) are shown in full view (center column), at the trailing edge (left column), and at the leading edge (right column). Also shown are the initial conditions of the bump for $U.x/$ (solid grey curve) and $H.x/$ (dashed grey curve). Eventually, the threshold crossings $u.a$ C $_{\mathrm{C}}^{a}; t/$ D h_0 C and $u.$ c C $^{c}; t/$ D h_0. Other parameters are h_0 D 0:04, D 0:1.

breather begins contracting once the threshold h becomes higher in amplitude than u at the pulse edge. The oscillation amplitude of the breathing solution decreases as decreases. Finally, in Fig. 12 we show an example of a shift perturbation destabilizing a bump in the case of stronger adaptation (larger). In this case the traveling pulse crosses threshold at five locations, rather than four points as in Fig. 10.

4. Discussion

In this paper we analyzed the linear stability of stationary bumps in a piecewise smooth neural field model with either synaptic depression or spike frequency adaptation. In both cases, stability analysis based on the construction of an Evans function breaks down in the high-gain limit. In the case of synaptic depression, we found that sufficiently strong synaptic depression can destabilize a bump that would be stable in the absence of synaptic depression; instabilities are dominated by shift perturbations that evolve into traveling pulses. The stability analysis assumed that the dominant instabilities were associated with non-oscillatory, separable solutions of the pseudo-linear Eqs.

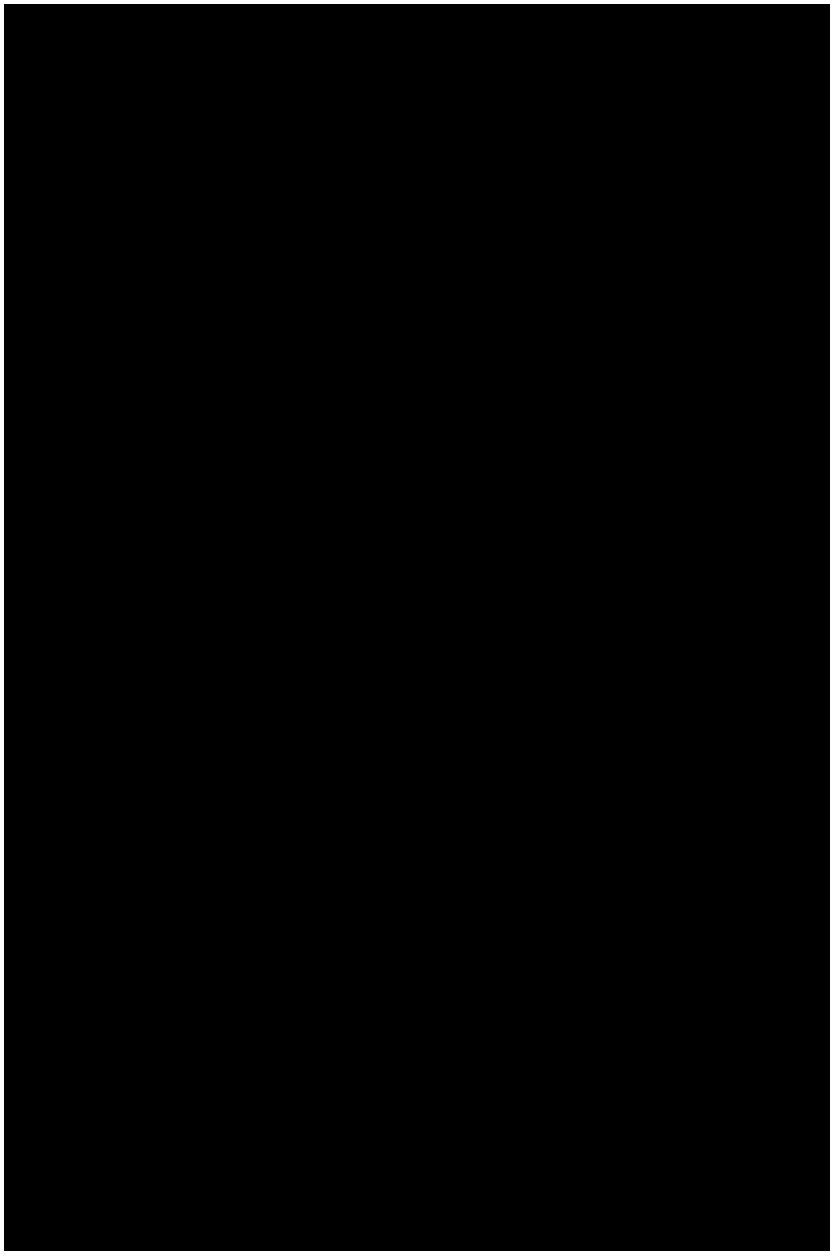

Fig. 11. Snapshots of a bump destabilizing to a breather at successive times t D 5; 6; 10; 20 (top to bottom) for D 1:2 and D 0:16. Both $u.x; t/$ (black curves) and $h.x; t/$

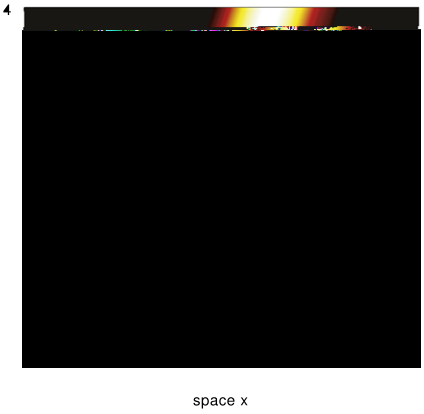

Fig. 12. Bump destabilizing to a traveling pulse for D 2:0; D 0:3. (a) Space time plot of the activity $u.x; t/$ evolving from an initial bump solution that is perturbed by a small rightward shift at t D 5. (b) Snapshot of perturbed solution $u.x; t/$ (black solid curve) and $h.x; t/$ (black squares) at time t D 20, along with initial profiles $U.x/$ (grey curve) and $H.x/$ (grey dashed curve). Eventually, the threshold crossing $u.a$ C $\frac{a}{C}; t/$ D h_0 C vanishes. Other parameters are h_0 D 0:04, D 0:1.

No. KUK-C1-013-4 granted by King Abdullah University of Science and Technology (KAUST). PCB was also partially supported by the Royal Society Wolfson Foundation.

References

[1] S. Funahashi, C.J. Bruce, P.S. Goldman-Rakic, Mnemonic coding of visual space in the monkey's dorsolateral prefrontal cortex, J. Neurophysiol. 61 (2) (1989) 331 349.
[2] E.K. Miller, C.A. Erickson, R. Desimone, Neural mechanisms of visual working memory in prefrontal cortex of the macaque, J. Neurosci. 16 (1996) 5154 5167.
[3] X.J. Wang, Synaptic reverberation underlying mnemonic persistent activity, Trends Neurosci. 24 (8) (2001) 455 463.
[4] H.S. Seung, How the brain keeps the eyes still, Proc. Natl. Acad. Sci. USA 93 (1996) 13339 13344.
[5] R. Ben-Yishai, R.L. Bar-Or, H. Sompolinsky, Theory of orientation tuning in visual cortex, Proc. Natl. Acad. Sci. USA 92 (1995) 3844 3848.
[6] S. Amari, Dynamics of pattern formation in lateral-inhibition type neural fields, Biol. Cybernet. 27 (2) (1977) 77 87.
[7] X.J. Wang, Synaptic basis of cortical persistent activity: the importance of NMDA receptors to working memory, J. Neurosci. 19 (21) (1999) 9587 9603.
[8] C.R. Laing, C.C. Chow, Stationary bumps in networks of spiking neurons, Neural Comput. 13 (2001) 1473 1494.
[9] S. Coombes, Waves, bumps, and patterns in neural field theories, Biol. Cybernet. 93 (2) (2005) 91 108.
[10] S. Coombes, M.R. Owen, Evans functions for integral neural field equations with heaviside firing rate function, SIAM J. Appl. Dyn. Syst. 34 (2004) 574 600.
[11] C.R. Laing, W.C. Troy, B. Gutkin, G.B. Ermentrout, SIAM J. Appl. Math. 63 (1) (2002) 62 67.
[12] C.R. Laing, W.C. Troy, PDE methods for nonlocal models, SIAM J. Appl. Dyn. Syst. 2 (3) (2003) 487 516.
[13] H. Werner, T. Richter, Circular stationary solutions in two-dimensional neural fields, Biol. Cybernet. 85 (2001) 211 217.
[14] S.E. Folias, P.C. Bressloff, Breathing pulses in an excitatory neural network, SIAM J. Appl. Dyn. Syst. 3 (3) (2004) 378 407.
[15]